BBA 46368

KINETICS OF THE FLUORESCENCE CHANGE AND P870 BLEACHING IN CHROMATOPHORES FROM *RHODOSPIRILLUM RUBRUM*

SHMUEL MALKIN AND BINAH SILBERSTEIN
Biochemistry Department, The Weizmann Institute of Science, Rehovot (Israel)
(Received April 11th, 1972)

SUMMARY

A parallel kinetic study on bacteriochlorophyll fluorescence change and P870 bleaching was performed on chromatophores from *Rhodospirillum rubrum* at different light intensities.

1. No direct correlation was found between P870 bleaching and the fluorescence rise, in contrast to previous results (L. N. Duysens and W. J. Vredenberg, *Nature*, 197 (1963) 355).

2. By analysing the kinetics in terms of a model in which two electron donors and two electron acceptors are participating it is shown that the variable fluorescence depends on a non-functional state of the reaction center, whether its electron acceptor is reduced or its electron donor is oxidized. There is a satisfactory agreement between the kinetic results and the theoretical kinetic curves derived on the basis of the above model, at different light intensities.

3. The theoretical model suggests a rate-limiting step on the electron-donor side, between a component C (cytochrome ?) and P870, with a first-order rate constant of about 0.83 s^{-1}. This rate-limiting step explains the fact that the rate of P870 bleaching is saturated at high light intensities. The rate of fluorescence increase is not saturated and obeys the $I \cdot t$ law, which is also in accord with the model.

INTRODUCTION

Early work suggested a close correlation between P870 bleaching and fluorescence yield increase in photosynthetic bacteria[1]. This correlation was thought to be due to the conversion of the reaction centers when their associated P870 molecules are oxidized. In this case P870 cannot act anymore as an electron donor and, as a result, the whole reaction center is unable to act as an excitation trap. Consequently, there is an increase in fluorescence from the bulk bacteriochlorophyll[2] which competes directly with the trapping of excitation.

Duysens and Vredenberg[1] fitted P870 bleaching and the fluorescence increase into a model in which the excitation trapping rate is proportional to the concentration of functional reaction centers. Clayton[3], however, found significant deviations from their model, at least under certain conditions. He suggested that the electron-acceptor part of the reaction center should also be taken into account. When the electron acceptor is in the reduced form the reaction center becomes non-functional in exactly

the same way as when the electron donor (P870) is oxidized. This view is amplified by the work of Parson[4], who showed for *Chromatium* chromatophores that after a single flash P870 is oxidized and rapidly (about 2 μs) rereduced, while the electron acceptor is reduced and remains reduced for several tenths of ms, during which the fluorescence yield is high[5].

A second point for consideration is the possibility of several photosystems operating together, independently or in cooperation. Sybesma and Fowler[6] and Sybesma and Kok[7] gave evidence for the existence of two kinds of reaction centers which drive the oxidation of two different cytochromes. Gromet-Elhanan and Feldman[8] showed the existence of two different types of electron-transfer reactions, showing different characteristics. It should be kept in mind that the fluorescence and P870 reaction may arise from different systems.

In view of the above considerations we undertook to reinvestigate the relation of P870 and the associated fluorescence rise under the same conditions and with different actinic and light intensities.

MATERIALS AND METHODS

The growth of *Rhodospirillum rubrum* cells and the isolation of chromatophores were as described by Briller and Gromet-Elhanan[9] and Gromet-Elhanan[10]. The chromatophores were divided into 2-ml ampules and were stored in liquid-nitrogen temperature. The storage medium contained 5 mM Tricine buffer (pH 7.5) in 50% glycerol. Electron transfer activities as well as fluorescence and P870 activities were found to remain practically intact for at least several months. The medium for the sample contained usually 80% sorbitol and was buffered to pH 7.5 by low concentration (10^{-5} M) of Tricine. Chromatophore concentration was $7 \cdot 10^{-6}$ M in bacteriochlorophyll, determined by using the extinction coefficient given by Clayton[11]. The above medium was chosen because it also allowed studies at low temperatures (> -80 °C) without freezing. The low-temperature studies will be reported separately.

Fluorescence and P870 were measured in the same apparatus (Aminco-Chance dual wavelength spectrophotometer) attached with a special cell holder with side illumination. The P870 measurement was carried out conventionally. For the fluorescence measurement a direct reading mode of the apparatus was used; the instrument measuring beam was turned off and the fluorescence was excited by the actinic beam. The fluorescence was isolated from the scattered actinic light by an interference filter (902 nm; close to the peak of the fluorescence emission spectrum) placed in front of the photomultiplier. The photomultiplier was of S-1 type (Hitachi-7102) and was cooled by stream of cold air to about -100 °C in order to reduce noise and dark current. The response time of the instrument is about 0.25 s for the P870 measurements and 1 ms for the fluorescence measurements.

Actinic light was provided from a Projector (Brown D-35) connected to a d.c. power supply. Appropriate filters were used to isolate a nearly monochromatic actinic beam. Here we demonstrate results for actinic light at 600 nm, but the general pattern of results was repeated also at other wavelengths.

RESULTS AND DISCUSSION

Fig. 1 depicts a typical on–off P870 bleaching pattern ($P870 \rightarrow P870^+$), the spectrum of which is given in the insert. In Fig. 2 a typical fluorescence rise pattern

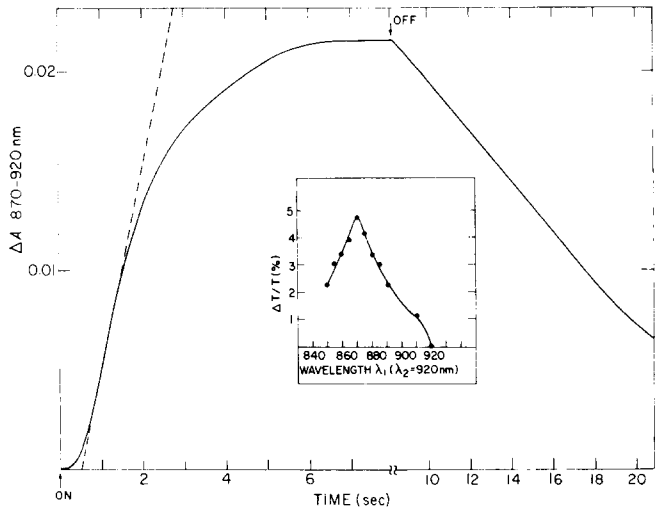

Fig. 1. An example for the kinetics of P870 bleaching and its dark backreaction of chromatophores suspension. Temperature, 25 °C. Light wavelength, 600 nm. Light intensity, 6 nEinsteins·$cm^{-2}\cdot s^{-1}$. Bacteriochlorophyll concentration, $7\cdot10^{-6}$ M.

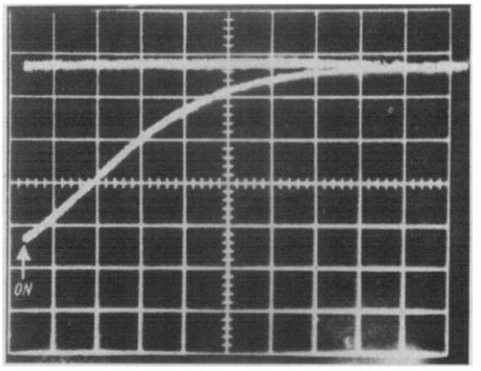

Fig. 2. Oscilloscopic photograph showing an example for fluorescence induction pattern of chromatophores suspension. At the onset of illumination the fluorescence excited by the actinic light takes the value F_0. During illumination the fluorescence rises to the final value (F_∞) which is marked by the following oscilloscopic sweep. Temperature, 25 °C. Light wavelength, 600 nm. Absorbed light intensity, 5 nEinsteins·$cm^{-2}\cdot s^{-1}$. Bacteriochlorophyll concentration, $7\cdot10^{-6}$ M. Time scale, 50 ms/division.

is shown. Comparing the two sets of data, for fluorescence and for P870, we decided to normalize the maximal change of both to 1. Fig. 3 shows both changes measured alternately in the same set-up as a function of time, at various light intensities. It may be observed that: P870 change and fluorescence changes are not correlated. As the light intensity increases the difference between them is extended significantly. The lack of correlation between P870 and the fluorescence is also seen in Fig. 4 which shows that the variable fluorescence quantum yield is not changed in the range of light intensities used, while the extent of P870 bleaching is diminished at low light intensities and becomes saturated only in the middle of the light intensity range.

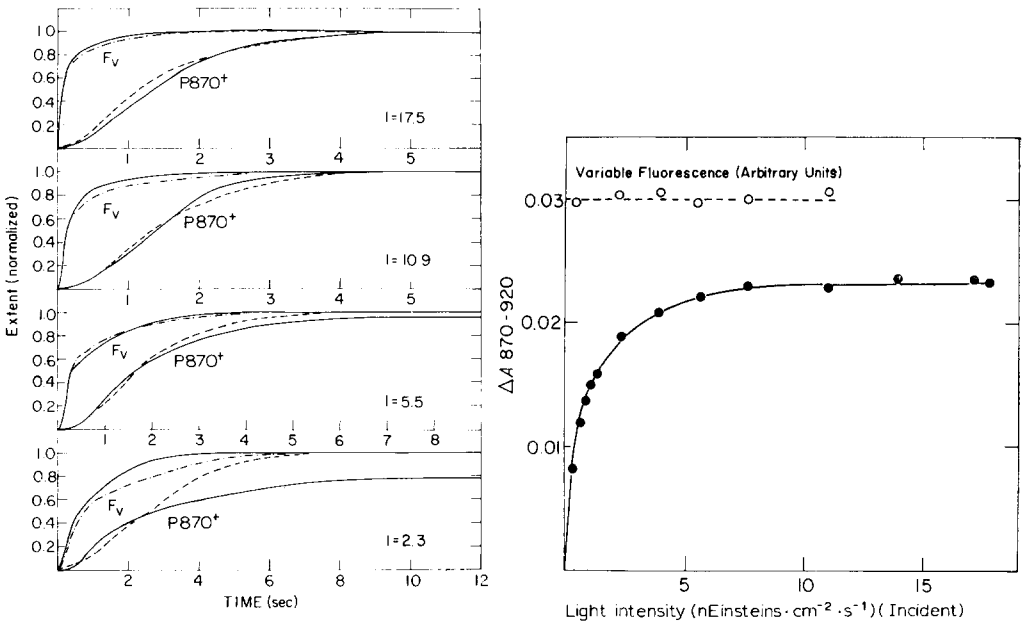

Fig. 3. Kinetics of P870 and fluorescence changes measured alternatively in the same set-up under the same experimental conditions, at different light intensities. The dashed curves are theoretical, calculated from Eqns 3 and 4 (*cf.* text). Temp., 25 °C. Light wavelength, 600 nm. Incident light intensities as indicated. Light absorption, 29 %. Bacteriochlorophyll concentration, $7 \cdot 10^{-6}$ M.

Fig. 4. Steady-state changes of both P870 and the variable fluorescence $(F_\infty - F_0)$ as function of the light intensity. Other details as in Fig. 3.

In order to study this lack of correlation in a more quantitative way we define the following parameters:

(a) The average time of reaction $\bar{t}$ defined by the area above each normalized curve:

$\bar{t}_F$ = average reaction time for the variable fluorescence rise, defined by the area above the normalized variable fluorescence $= \int_0^\infty (1 - F_v)\mathrm{d}t$

$\bar{t}_p$ = average reaction time for the P870 $= \int_0^\infty (1 - \mathrm{P870^+})\mathrm{d}t$

(b) The maximum rate, R, obtained for P870 bleaching at each light intensity: Since there is a typical lag in P870 bleaching upon the onset of illumination, the maximum rate is obtained not at $t = 0$ but at some intermediate time. On the normalized P870 curve this rate has dimensions s^{-1}. In Fig. 1 we drew tangent to the P870 bleaching showing the maximum slope, from which R is calculated:

R = maximal rate for P870 bleaching = max. $\left(\frac{\mathrm{dP870^+}}{\mathrm{d}t}\right)$

A qualitative inspection (Fig. 3) shows that while the fluorescence rise is faster as

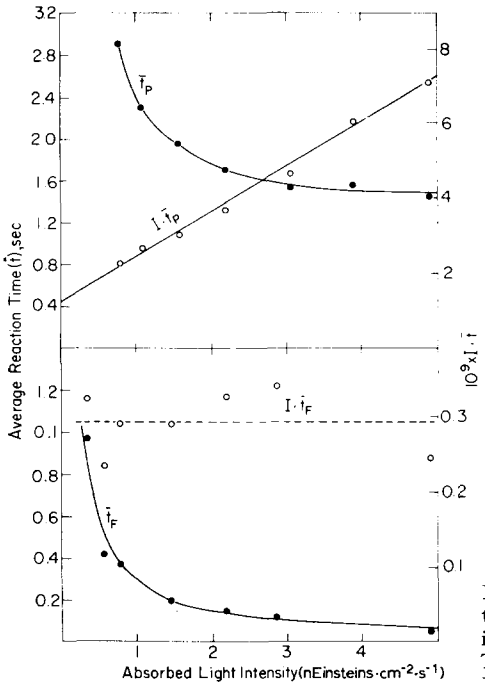

Fig. 5. Plots of the average reaction times and the products of the reaction times and the light intensity as a function of the light intensity. Top: $\bar{t}_p$ (left scale) and $I \cdot \bar{t}_p$ (right scale) *vs* I. Bottom: $\bar{t}_F$ (left scale) and $I \cdot \bar{t}_F$ (right scale) *vs* I. Experimental conditions, as in Fig. 3. Fluorescence and P870 data cannot be compared quantitatively in this figure, since they were obtained in different series of experiments.

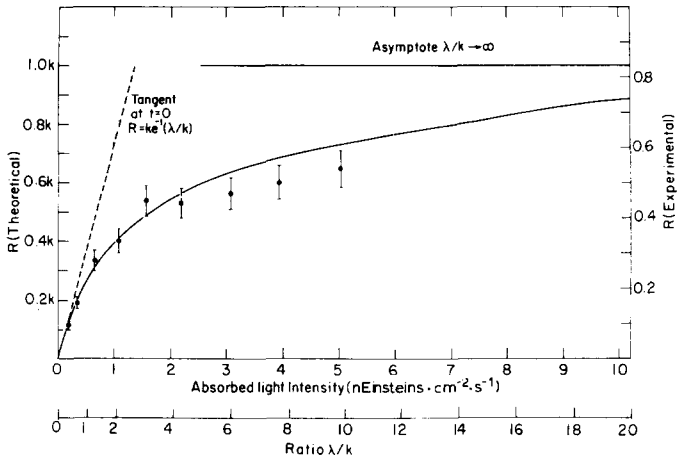

Fig. 6. Experimental points and theoretical (continuous curve) plots of the maximal rate of P870 bleaching *vs* the light intensity, after adjustment of the theoretical scale to the experimental scale (*cf.* text). Experimental scales: left ordinate and top abscissa. Theoretical scales: right ordinate and bottom abscissa.

the light intensity increases, the P870 bleaching tends toward saturation. Fig. 5 emphasizes this conclusion in a quantitative way: $\bar{t}_F$ is proportional to I^{-1} ($I \cdot \bar{t}_F = \text{const.}$) while $\bar{t}_p$ tends to a limit as I increases ($I \cdot \bar{t}_p$ increases linearly with I). R behaves similar to $\bar{t}_p$ and tends to a saturation value as I increases (Fig. 6).

Another interesting feature is the appearance of a typical lag in P870 oxidation which was previously noted by Beugeling and Duysens[12] for a different organism (*Chromatium*). The lag was ascribed[13] to the fast electron transfer from a cytochrome to $P870^+$, confirmed by laser flash experiments[4]. It is therefore suggested that the lag in our case is due too to a fast reaction between P870 and the electron donor (cytochrome probably) which rereduces P870 during the lag period, until it is appreciably oxidized and only then P870 oxidation starts. Parson[14], however, showed that in his chromatophore preparation from *R. rubrum* the $P870^+$ rereduction after a brief flash was relatively slow and only its fast phase (extent approx. 20%; time approx. 100 μs) was correlated to a cytochrome oxidation. In whole cells of *R. rubrum*, on the other hand, the rereduction of $P870^+$ was quite fast[15] (approx. 25 μs). It seems that the coupling between $P870^+$ and cytochrome is sensitive to destruction in the chromatophore preparation from *R. rubrum*. However, in such a case a lag in P870 oxidation by continuous light is not expected. In this study a more delicate method for chromatophore preparation was used, which may be sufficient to reserve the coupling between P870 and its electron donor*. As a first approximation we shall therefore try to explain our results in terms of two donors–two acceptors scheme:

$$\underset{(A)}{CPXY} \xrightarrow{h\nu} \underset{}{(CP^+X^-Y)} \rightarrow \underset{(B)}{C^+PX^-Y} \xrightarrow{k} \underset{(C)}{C^+PXY^-} \xrightarrow{h\nu} \underset{(D)}{C^+P^+X^-Y^-} \qquad \text{(i)}$$

(C = cytochrome or anyother electron donor, P = P870, X = primary electron acceptor, Y = secondary electron acceptor).

In the above scheme we assume: (a) The electron transfer time between C and P^+ is fast compared to our time of measurement so that the momentary concentration of CP^+X^-Y can be neglected. (b) The quantum yields of the first and last (photochemical) steps are equal, as these are in fact the same photochemical reactions (we neglect secondary effects of C^+ and Y^- on the quantum yield).

The original model of Duysens and Vredenberg[1] does not fit the data presented so far. Therefore, we did not use their kinetic equations. Instead, we assume first-order rate laws for all the species present**. For the light reactions we assume the model of independent units[16,17], so that the rate of photoconversion is proportional to the light which is directly absorbed in the appropriate units.

Taking the above assumptions and considerations into account, we obtain from Scheme i the following:

$$\frac{dA}{dt} = -\frac{\phi I A}{A_0} = -\lambda A \qquad \text{(1a)}$$

A–D = concentrations of the species A–D, defined in Eqn i; $A_0 = A + B + C + D$; ϕ = quantum yield; I = absorbed light intensity; $\lambda = \phi I/A_0$ = absorbed light intensity in a scale of "active" quanta per reaction center per unit of time.

$$\frac{dB}{dt} = \lambda A - kB \qquad \text{(1b)}$$

* We could not check the reaction Cyt. $P870^+ \rightarrow$ Cyt.$^+$ P870 directly, in the absence of appropriate equipment.

** The exact form of the rate law does not seem very crucial, and the convenience of calculation and presentation is more important.

$$\frac{dC}{dt} = kB - \lambda C \tag{1c}$$

$$\frac{dD}{dt} = \lambda C \tag{1d}$$

The solution is obvious:

$$A = A_0 e^{-\lambda t} \tag{2a}$$

$$B = \frac{kA_0}{k-\lambda}(e^{-\lambda t} - e^{-kt}) \tag{2b}$$

$$C = \frac{k\lambda A_0}{(k-\lambda)^2}(e^{-\lambda t} - e^{-kt}) + \frac{k\lambda A_0}{k-\lambda} t e^{-\lambda t} \tag{2c}$$

$$D = A_0 - (A + B + C) \tag{2d}$$

The normalized variable fluorescence will be taken as equal to the fraction of non-functional centers $(B+D)/(A+B+C+D)$ and $P870^+$ will be taken as equal to $D/(A+B+C+D)$. Hence:

$$\text{(Normalized) } F_v = 1 - \left(1 - \frac{k\lambda}{(k-\lambda)^2}\right) e^{-\lambda t} - \frac{k\lambda}{k-\lambda} t e^{-\lambda t} - \frac{k\lambda}{(k-\lambda)^2} e^{-kt} \tag{3}$$

$$\text{(Normalized) } P870^+ = 1 - \frac{k^2 - 2k\lambda}{(k-\lambda)^2} e^{-\lambda t} - \frac{k\lambda}{k-\lambda} t e^{-\lambda t} - \frac{\lambda^2}{(k-\lambda)^2} e^{-kt} \tag{4}$$

Manipulating on the above results for P870 and the fluorescence we get for the average reaction times:

$$\bar{t}_F = \int_0^\infty (I - F_v)dt = \frac{2}{\lambda} = \frac{2A_0}{\phi I} \quad \text{or} \quad I \cdot \bar{t}_F = \frac{2A_0}{\phi} = \text{const.} \tag{5}$$

$$\bar{t}_p = \int_0^\infty (I - P870^+)dt = \frac{2}{\lambda} + \frac{1}{k} \quad \text{or} \quad I \cdot \bar{t}_p = \frac{2A_0}{\phi} + \frac{I}{k} \tag{6}$$

The results (5) and (6) confirm theoretically what had been observed in the experiment (Fig. 5). By plotting $I \cdot \bar{t}_F$ *vs* I we get a constant $(2A_0/\phi)$. Similarly, by plotting $I \cdot \bar{t}_p$ *vs* I we get a straight line with an intercept of $2A_0/\phi$ and a slope of $1/k$. (The set of data for the fluorescence was taken from a different series of experiments, so that the parameters for the fluorescence and for P870 cannot be compared directly in Fig. 5. All the other experiments, including the P870 experiments in Fig. 5, are from the same series.)

R vs I: It is not easy to express R analytically in terms of I (and k). We shall express R precisely only for the three special cases: (a) for small light intensities, where we shall find that R is proportional to I; (b) for the special value of the light intensity when $\lambda = k$; (c) for very high light intensities, where we find that R tends to a saturating value.

Let us derive the expression for $dP870^+/dt$, from Eqn 4:

$$\frac{dP870^+}{dt} = -\frac{k\lambda^2}{(k-\lambda)^2} e^{-\lambda t} + \frac{k\lambda^2}{k-\lambda} t\, e^{-\lambda t} + \frac{k\lambda^2}{(k-\lambda)^2} e^{-kt} \tag{7}$$

(a) For low light intensity, $\lambda \ll k$, we may neglect λ in comparison to k in Eqn. 7. This simplified form of Eqn 7 is:

$$\frac{dP870^+}{dt} \approx \lambda^2 t\, e^{-\lambda t} - \frac{\lambda^2}{k}(e^{-\lambda t} - e^{-kt}) \tag{7a}$$

$\lambda \ll k$

The contribution of the term with e^{-kt} diminishes very fast with t compared to the term with $e^{-\lambda t}$. Generally, with the exception of times close to $t = 0$, Eqn 7a is further approximated by:

$$\frac{dP870^+}{dt} = \left(\lambda^2 t - \frac{\lambda^2}{k}\right) e^{-\lambda t} \tag{7a'}$$

$\lambda \ll k, \quad t \gg \lambda/k$

Going through the standard procedure for equating the derivative of Eqn 7a' to zero, one gets the straightforward answer for $R = \text{max.}\ (dP870^+/dt)$

$$R = e^{-1}\lambda\, e^{-\lambda/k} \to e^{-1}\lambda = \frac{e^{-1}\phi}{A_0} I \tag{8a}$$

$\lambda/k \to 0$

(b) For the special case $\lambda = k$ Eqn 7 is transformed to:

$$\frac{dP870^+}{dt} = \frac{k^3}{2} t^2\, e^{-kt} \tag{7b}$$

$\lambda = k$

and

$$R = \text{max.}\left(\frac{dP870^+}{dt}\right) = 2k\, e^{-2} \tag{8b}$$

$\lambda = k$

(c) For the case of high light intensities, such that $\lambda \gg k$ we get from Eqn 7 by neglecting k compared to λ:

$$\frac{dP870^+}{dt} \approx k(e^{-kt} - e^{-\lambda t} - \lambda t\, e^{-\lambda t}) \tag{7c}$$

$\lambda \gg k$

As λ increases the function e^{-kt} decreases only little with time compared to the re-

duction of both $e^{-\lambda t}$ and $\lambda t e^{-\lambda t}$, and hence most of the time a good approximation to Eqn 7c would be:

$$\frac{dP870^+}{dt} \approx k\, e^{-kt} \qquad (7c')$$

$$\lambda \gg k, \quad t \gg k/\lambda$$

Hence: $R \leqslant k$, the difference between R and k approaching zero as $\lambda/k \to \infty$.

In a further study of R *vs* I a theoretical plot was made by the following simple transformation of Eqn 7. Upon writing Eqn 7 in terms of the parameter λ/k we get:

$$\frac{dP870^+}{dt} = k\left[\frac{(\lambda/k)^2}{(1-\lambda/k)^2} e^{-\lambda t} + \frac{\lambda/k}{1-\lambda/k}\lambda t\, e^{-\lambda t} + \frac{(\lambda/k)^2}{(1-\lambda/k)^2} e^{-(\lambda/k)^{-1}\lambda t}\right]$$

The expression inside the brackets is $dP870^+/dt$, in units of k, expressed in terms of the parameter λ/k and the variable λt. We have plotted its dependence on λt for various chosen values of λ/k and found its maximal value for each value of λ/k. The result is R, in units of k, as function of λ/k, which is plotted in Fig. 6 (solid line, left and bottom scales).

From the above considerations, and the theoretical plot of Fig. 6 we predict that R starts as a linear function of I, with a slope $e^{-1}\phi/A_0$. As I increases the curve bends down until it reaches a saturation value k.

The values of the parameters k and A_0/ϕ may be obtained by several methods: (1) from the slope ($= 1/k$) and intercept ($= 2A_0/\phi$) of the plot $I \cdot \bar{t}_p$ *vs* I (Eqn 6); (2) from the initial slope ($= e^{-1}\phi/A_0$) of R *vs* I (Eqn 8a); (3) from the light intensity I_1 at which the ratio of R to the value extrapolated from the initial slope of R *vs* I is $2ke^{-2}/ke^{-1} = 2e^{-2}$ (ratio of Eqn 8b to Eqn 8a). At this point $k = \lambda$ and hence $k = \phi\, I_1/A_0$ (for this calculation we may use the value for A_0/ϕ obtained by methods (1) or (2) above). The results of these calculations are shown in Table I, and their consistency demonstrate the agreement of $P870^+$ kinetics to the reaction scheme (i) and Eqn 4.

TABLE I

SUMMARY OF THE KINETIC PARAMETERS OF THE CPXY SCHEME

Method/parameter	k (s^{-1})	A_0/ϕ (*nmole/cm*^{3})	ϕ
From $I \cdot t_p$ *vs* I (Eqn 6)	0.83	0.62	0.35
From initial slope of R *vs* I (Eqn 8a)		0.55–0.68	
From the light intensity I_1, where $\lambda = k$ (Eqns 8b and 8a)	≈0.9		

To further emphasize this agreement we chose the values of k and A_0/ϕ obtained from $I \cdot \bar{t}_p$ *vs* I in order to adjust the scale of the theoretical R *vs* λ/k curve to the experimental R *vs* I curve (Fig. 6). This was done simply by adjusting the abscissa scale in Fig. 6 so that $\lambda/k = (\phi/A_0 k)I \approx 1.96\, I$, and the ordinate scale to $k \approx 0.83$. The experimental points along the curve follow the theoretical curve quite closely.

There is a small deviation at high light intensity, which may be due to instrumental reasons (the time of the reaction begins to approach the time resolution of the instrument).

As an additional test we have calculated theoretical kinetical curves for both P870 (Eqn 4) and the fluorescence rise (Eqn 3), using the values of A_0/ϕ and k obtained in Table I. The result is shown and compared to the experimental results in Fig. 3. There is a reasonable agreement between the theoretical and experimental curves. Deviations occur at the low light intensity range in which dark backreactions (not accounted for in the theory) are of considerable influence. These backreactions cause $P870^+$ to approach a lower steady state (≈ 0.8) at $I = 2.3$ nEinsteins$\cdot cm^{-2}\cdot s^{-1}$ (Fig. 3, bottom).

From the value $A_0/\phi \approx 0.62$ nmole/cm^3 (Table I), and a value for A_0 (0.215 nmole/cm^3) obtained from the maximal extent of P870 bleaching, using an ε value of $10^{-5}\ M^{-1}\cdot cm^{-1}$, we get a value for $\phi \approx 0.35$. This is the quantum yield of the primary charge separation in a functional unit. This number is in agreement with the value of Vredenberg[18]. However, one cannot attach special significance to this value since values of ϕ approaching 1 have been claimed[19].

The characteristic time for the rate limiting step of the stop reaction (*i.e.* the reaction which limits our system to only 4 electron carriers) must be evidently much longer than our value of k. An estimate for it may be given from the time of the back dark reduction of P870, which is in the order of 10–20 s (*cf.*, *e.g.* Fig. 1, off-reaction). The steady-state rate of electron transfer cannot exceed 0.1–0.2 e^- equiv per mole of reaction centers (10–20 μequiv/mg bacteriochlorophyll per h) obtained by using the ratio P870/bacteriochlorophyll = 1:35, measured in our samples and with agreement with previous estimates[20]). The above rate is quite small compared to the rates obtained with biochemical oxidoreduction reactions and photophosphorylation (usually in the order of 100 specific activity). The P870 and fluorescence reactions should be investigated in a variety of reaction conditions, and be correlated to steady-state electron transfer.

If it is accepted that P870 bleaching is a primary reaction, the mere fact that its rate of bleaching is saturated at high light intensity almost leads us to assume the existence of a rate-limiting step on the e^--acceptor side. (A rate limiting step on the e^--donor side cannot cause a rate saturation (*cf.* Appendix).) Our model, described by Reaction i is a minimal model, with respect to the number of electron carriers. With more electron carriers, however, we expect a longer lag in P870 bleaching (*cf.* Appendix). Reaction scheme (i) seems to fit the experimental data better than any other feasible scheme.

Our results do not throw light on the feasibility of the existence of several photochemical systems, since they are consistent with the fluorescence and P870 originating from the same system.

APPENDIX

Analysis of reaction models for electron transfer, when the primary electron donor is observed

As the most general scheme we assume the existence of pools of secondary

electron donors (C_i) and electron acceptors (Y_i), reacting respectively with the primary electron carriers P870 (denoted P) and X

$$\begin{array}{c} h\nu \\ \downarrow \\ \longrightarrow \text{ electron flow} \\ C_n \ldots C_2 C_1 P \mid X Y_1 Y_2 \ldots Y_m \end{array}$$

The electron-transfer reaction is equivalent to the filling of the above pools, with electrons (right side) or "holes" (left side). We assume that the electron-transfer reaction is irreversible at each step so that if all reaction steps are fast compared to the production of electrons and holes the pools are filled in order from the terminal to the primary ones. The reaction stops when either one of the right or the left pools is completely filled.

Obviously if the sum total equivalent value of the pools on each side is significantly larger than that of the other side, the primary electron carrier at this side will remain unreacted. Since we observe the oxidation of P, we may conclude that the equivalent value of the oxidizing side is smaller than or equal to the equivalent value of the reducing side. During the filling of the C pools P oxidation is not observed or is small (lag period). This lag period is evidently proportional to the total size of the C pools (*cf.* later). When P oxidation finally commences its kinetics would correspond to the isolated system:

$$PX \rightarrow P^+X^- \text{ (when the } Y_{pool} = C_{pool}) \text{ or } PX \rightarrow P^+X \text{ (when the } Y_{pool} > C_{pool})$$

both are primary reactions and cannot be saturated at ordinary intensities*.

As the light intensity increases, the rate of production of electron and "holes" increases and a certain step becomes rate limiting. Such a step may be regarded as a "leak" if its rate is much smaller than the electron production rate. The effect of such a step in the e^--donor side would be to effectively decrease the C pools, hence the lag period would decrease, but the kinetics of P oxidation when it commences would again correspond to the system $PX \rightarrow P^+X^-$, or $PX \rightarrow P^+X$, and again will not be saturated.

On the other hand, a rate-limiting step in the e^--acceptor side will effectively decrease the size of the Y pool. If it is located in a place between Y_s and Y_{s+1} such

$$\sum_{i=1}^{s} Y_i < \sum_{i=1}^{n} C_i,$$

X will be reduced during the lag period, since X will be filled before all the C pools are filled. When P oxidation commences, its rate would be limited by the availability of oxidized unfilled X. P oxidation rate would be therefore determined by the "leak" of electrons in the rate-limiting step reaction, which is independent of the light intensity. In this case P oxidation will be saturated.

* A primary reaction can be saturated only if the light input rate is much higher than the preceeding dark reaction rates. Typically, these dark reactions involve excited state intermediates with life times of the order of 10^{-4} (triplets) to 10^{-9} (singlets) s. Laser flash experiments (ref. 4) indicate that the limiting dark reaction times must be less than 10^{-6} s. Saturating light intensity would be in the order of $\gtrsim 10^6$ photons/s per reaction center, which is 10^6 stronger than used in our case.

To see this in a quantitative way one can consider two extreme models:

(a) Independent units model, in which the components P, X, C_i, Y_i, are arranged in a linear way and react with each other in the order indicated by the scheme above, but a specific molecule can react with its own partner only by a monomolecular reaction scheme.

(b) Bimolecular reaction model, in which all components react in the same order but each molecule of one kind can react with any molecule of a second kind. Any mixed model will give results which are between the results derived from the above two models.

The formulation of the reactions scheme according to the model (a), assuming the rate-limiting step in the oxidizing side between C_h and C_{h+1}, is:

Species (Rate limiting step)

$$(A_0) \quad C_n...C_{h+1} \mid C_h...C_1\,PXY_1...Y_n \xrightarrow{h\nu}$$

$$(A_1) \quad C_n...C_{h+1} \mid C_h^+...C_1\,PXY_1...Y_n^- \xrightarrow{h\nu}$$

$$(A_2) \quad C_n...C_{h+1} \mid C_h^+C_{h-1}^+...C_1\,PXY_1...Y_{n-1}^-Y_n^- \xrightarrow{h\nu}$$

$$\xrightarrow{h\nu}$$

etc.

$$(A_h) \quad C_n...C_{h+1} \mid C_h^+...C_1^+\,PXY_1...Y_{n-h+1}^-...Y_n^- \xrightarrow{h\nu}$$

$$(A_{h+1}) \quad C_n...C_{h+1} \mid C_h^+...C_1^+\,P^+XY_1...Y_{n-h}^-...Y_n^-$$

In short form:

$$A_0 \xrightarrow{h\nu} A_1 \xrightarrow{h\nu} A_2 \xrightarrow{h\nu} ... \xrightarrow{h\nu} A_{h+1}$$

(the leak to $C_{h+1}....C_n$ is neglected).

The expression for P^+ is:

$$\text{Normalized } P^+ = \frac{A_{h+1}}{\sum_{i=0}^{h+1} A_i} \qquad \text{(App. 1)}$$

Assuming a first-order rate low for each species, and equal quantum yields for each step we get:

$$\frac{dA_0}{dt} = -\lambda A_0 \qquad \frac{dA_l}{dt} = -\lambda(A_l - A_{l-1}) \qquad \frac{dA_{h+1}}{dt} = \lambda A_h \qquad \text{(App. 2)}$$

$$0 < l < h + 1$$

where λ is the rate of production of electrons (holes) per reaction center. The solution for the above equations is quite standard. The results for $A_{h+1}/\Sigma A_i$ = normalized P^+ is:

$$P^+ = 1 - \left(1 + \lambda t + \frac{\lambda^2 t^2}{2!} + \frac{\lambda^3 t^3}{3!} + ... + \frac{\lambda^h t^h}{h!}\right) e^{-\lambda t} \qquad \text{(App. 3)}$$

Analysis of this expression shows: (a) P^+ is not saturated as λ increases. This is shown by the fact that t appears only in combination with λ. (b) A rate-limiting step between C_h and C_{h+1} causes the lag to decrease, and P oxidation to be accomplished relatively faster, compared to a rate-limiting step or stop reaction at a further point. If we define the lag period, T, as the time from $t = 0$ to the point where P is bleached at a maximal rate we directly get from Eqn (App. 3):

$$\text{(Lag period)} \quad T = h/\lambda \qquad \text{(App. 4)}$$

The lag period is therefore proportional to the number of equivalents from P to the rate-limiting points.

Exactly the same result is obtained by a bimolecular reaction model; here the terminal C pools must be filled completely before P oxidation commences. Hence the expression P^+ would be:

$$\begin{aligned} P^+ &= 0 && \text{for } \lambda t \leqslant h \\ P^+ &= 1 - e^{-(\lambda t - h)} && \text{for } \lambda t > h \end{aligned} \qquad \text{(App. 5)}$$

The lag period is given again by formula (App. 4), although the exact shape of P^+ *vs* t is different. Here the rate of P^+ is strictly zero for $t > h/\lambda$, and jumps discontinuously at $t = h/\lambda$ to a maximal value λ. Based on this, our experimental results fit better the independent units model (a).

A rate-limiting step in the *e*-acceptor side would lead to a similar reaction scheme as above, but the reduction of X will be completed before the oxidation of P commences, as follows:

Species

$$(B_0) \qquad C_n \ldots C_1\, PXY_1 \ldots Y_g \,|\, Y_{g+1} \ldots Y_n \xrightarrow{h\nu}$$

$$(B_1) \qquad C_n^+ \ldots C_1\, PXY_1 \ldots Y_g^- \,|\, Y_{g+1} \ldots Y_n \xrightarrow{h\nu}$$

etc.

$$(B_g) \qquad C_n^+ \ldots C_{n-(g+1)}^+ \ldots C_1\, PXY_1^- \ldots Y_g^- \,|\, Y_{g+1} \ldots Y_n \xrightarrow{h\nu}$$

$$(B_{g+1}) \qquad C_n^+ \ldots C_{n-g}^+ \ldots C_1\, PX^- Y_1^- \ldots Y_g^- \,|\, Y_{g+1} \ldots Y_n$$

In short form:

$$B_0 \xrightarrow{h\nu} B_1 \xrightarrow{h\nu} B_2 \xrightarrow{h\nu} B_3 \xrightarrow{h\nu} \ldots \xrightarrow{h\nu} B_{g+1}$$

The oxidation of the rest of the pools $C_{n-(g+1)}$– P would continue slowly with the rate of the "leak" at Y_g.

$$B_{g+1} \xrightarrow{k} B_{g+2} \xrightarrow{k} \ldots \xrightarrow{k} B_{n+1}$$

where

$$B_{g+2} = C_n^+ \ldots C_{n-(g-1)}^+ C_{n-(g-2)} \ldots C_1\, PX^- Y_1^- \ldots Y_g^- \,|\, Y_{g+1} \ldots Y_{n-1} Y_n^-$$

$$B_{g+3} = C_n^+ \ldots C_{n-(g-2)}^+ C_{n-(g-3)} \ldots C_1\, PX^- Y_1^- \ldots Y_g^- \,|\, Y_{g+1} \ldots Y_{n-2} Y_{n-1}^- Y_n^-$$

$$B_{n+1} = C_n^+ \ldots C_1^+\, P^+ X^- Y_1^- \ldots Y_n^-$$

The results for $B_{n+1}/\Sigma B_i$ = normalized P^+, for $\lambda \gg k$ is approximately given by an expression similar to App. 3.

$$P^+ = 1 - \left(kt + \frac{k^2t^2}{2!} + \ldots + \frac{k^{n-(g+1)}t^{n-(g+1)}}{[n-(g+1)]!}\right)e^{-kt} \qquad \text{(App. 6)}$$

Now P^+ is saturated(!). As λ increases P^+ approaches more closely to the above expression (App. 6) which does not depend on λ.

The lag period is given in this case by the following (approximate) equation:

$$T = [n-(g+1)]/k \qquad \text{(App. 7)}$$

The bimolecular model (b) gives, as before, a similar conclusion:

$$P^+ = 0 \qquad \text{for } t < \frac{g+1}{\lambda} + \frac{n-(g+1)}{k} = \tau$$
$$P^+ = 1 - e^{k(t-\tau)} \text{ for } t < \tau \qquad \text{(App. 8)}$$

Again because of the sudden change in rate predicted by this model we prefer the independent units model (a).

REFERENCES

1 L. N. Duysens and W. J. Vredenverg, *Nature*, 197 (1963) 355.
2 R. K. Clayton, *Photochem. Photobiol.*, 5 (1966) 679.
3 R. K. Clayton, *Photochem. Photobiol.*, 5 (1966) 807.
4 W. W. Parson, *Biochim. Biophys. Acta*, 153 (1968) 248.
5 W. W. Parsod, *Biochim. Biophys. Acta*, 189 (1969) 384.
6 C. Sybesma and C. E. Fowler, *Proc. Natl. Acad. Sci. U.S.*, 61 (1968) 1343.
7 C. Sybesma and B. Kok, *Biochim. Biophys. Acta*, 180 (1969) 410.
8 Z. Gromet-Elhanan and N. Feldman, in *2nd Int. Congr. of Photosynthesis Research, Stresa, Italy, 1971*, in the press.
9 S. Briller and Z. Gromet-Elhanan, *Biochim. Biophys. Acta*, 205 (1970) 263.
10 Z. Gromet-Elhanan, *Biochim. Biophys. Acta*, 223 (1970) 263.
11 R. K. Clayton, in H. Gest, A. San Pietro and L. P. Vernon, *Bacterial Photosynthesis*, Antioch Press, Yellow Springs, Ohio, 1963, p. 495.
12 T. Beugeling and L. N. M. Duysens, in J. B. Thomas and J. C. Goedheer, *Currents in Photosynthesis*, Donker, Rotterdam, 1966, p. 49.
13 L. N. M. Duysens, in J. B. Thomas and J. C. Goedheer, *Currents in Photosynthesis*, Donker, Rotterdam, 1966, p. 49.
14 W. W. Parson, *Biochim. Biophys. Acta*, 131 (1967) 154.
15 B. Chance and D. De Vault, *Abstr. Biophys. Soc. Meet. WH$_4$, San Francisco*, (1965) 56.
16 S. Malkin, *Biochim. Biophys. Acta*, 126 (1966) 433.
17 S. Malkin, *Biophys. J.*, 9 (1969) 489.
18 W. J. Vredenberg, *Spectrophotometric Studies on Primary and Associated Reactions in Photosynthesis*, Thesis, Leiden, 1965, p. 27.
19 P. A. Loach, *Biochemistry*, 7 (1968) 2642.
20 R. K. Clayton, *Photochem. Photobiol.*, 1 (1962) 201.